# Evolution of thermal physiology alters predicted species distributions under climate change

Sara J.S. Wuitchik[1,†,*], Stephanie Mogensen[1], Tegan N. Barry[1], Antoine Paccard[2,‡], Heather A. Jamniczky[3], Rowan D.H. Barrett[2,§], and Sean M. Rogers[1,4,§]

[1]Department of Biological Sciences, University of Calgary, 2500 University Dr NW, Calgary, AB, T2N 1N4, CANADA

[2]Redpath Museum and Department of Biology, McGill University, 845 Sherbrooke St W, Montreal, QC, H3A 0G4, CANADA

[3]Department of Cell Biology & Anatomy, Cumming School of Medicine, University of Calgary, 3330 Hospital Dr NW, Calgary, T2N 4N1, CANADA

[4]Bamfield Marine Sciences Centre, 100 Pachena Rd, Bamfield, BC, V0R 1B0, CANADA

[§]equal co-senior authors

***Corresponding author: Sara J.S. Wuitchik**

E: sjswuit@g.harvard.edu

T: 857-292-9977



†Present affiliations: Informatics Group, Harvard University, 38 Oxford St, Cambridge, MA, 02138, USA & Department of Biology, Boston University, 5 Cummington Mall, Boston, MA, 02215, USA
‡Present affiliation: McGill University Genome Center, 740 Dr Penfield Avenue, Montreal, QC, H3A 1A5, Canada

22 Species distribution models (SDMs) are widely adopted to predict range shifts but can be
23 unreliable under climate change scenarios[1] because they do not account for evolution. The
24 thermal physiology of a species is a key determinant of range[2,3] but the impact of thermal trait
25 evolution on SDMs has not been addressed. We identified a genetic basis for physiological traits
26 that evolve in response to temperature change in threespine stickleback. Using these data, we
27 created geographic range projections under two climate change scenarios where trait data was
28 either static ('no evolution' model), allowed to evolve in agreement with published evolutionary
29 rates for the trait ('evolution' model)[4], or allowed to evolve with the rate of evolution scaled in
30 association with the variance that is explained by QTL ('PVE' model). Here, we show that
31 incorporating these traits and their evolution into SDMs substantially altered the predicted ranges
32 for a widespread panmictic marine population, with increases in area of over 7-fold. Evolution-
33 informed SDMs should therefore improve the precision of forecasting range dynamics under
34 climate change, thereby aiding in their application to management and the protection of
35 biodiversity[5–7].

36 Temperature is a powerful driver of global biogeography and organism distributions
37 frequently reflect temperature gradients in both aquatic and terrestrial habitats[8]. Many species
38 adopt thermal strategies (such as thermoregulation or acclimation) that determine their thermal
39 niche[9–11] and thermal traits can provide a target for directional selection if the environment
40 changes to include temperatures outside the range encompassed by the thermal niche. Adaptation
41 may thus permit species to persist at temperatures that would have previously led to
42 extirpation[12,13]. Under moderate climate change scenarios, mean global oceanic temperature is
43 predicted to increase in excess of 2°C by the end of the century[14], with more extreme changes
44 predicted in localized regions[15]. Predicting species distribution patterns under climate change

45 therefore requires data for temperature-associated adaptive trait evolution, which can vary by
46 species and population. While there have been recent steps to incorporate theoretical trait
47 evolution into SDMs[3], to date, no model has used empirical estimates of evolutionary rate to
48 inform predictions about future species distributions.

49 Due to widespread phenotypic variation[16], genomic resources[17], the availability of
50 temperature-associated ecological and evolutionary trait data[4], and the ability to artificially breed
51 multiple hybrid generations in a common garden lab environment, threespine stickleback fish
52 (*Gasterosteus aculeatus*, Fig. 1a) are a useful vertebrate species for understanding the impact of
53 adaptation on range dynamics under climate change. Here, we incorporate the specific capacity
54 of marine populations to adapt their physiology to rapidly changing climate conditions to
55 characterize how adaptive trait variation affects projections of species range distributions under
56 climate change[18].

57 **Results**

58 We collected and reared wild marine and freshwater stickleback from two marine and
59 two freshwater locations (Fig. 1b). These stickleback exhibited a wide thermal tolerance range
60 bounded by a mean CTmin of 2.09 °C (+/- 1.13 °C SD) and a mean CTmax of 30.4 °C (+/- 2.64
61 °C SD)(Fig. 1c) and also tolerated a wide range of temperatures within which there was no
62 observable stress response (5.0 – 25.0 °C). To determine if these measured thermal traits have a
63 genetic basis and could therefore be subject to adaptive evolution, we raised hybrid marine-
64 freshwater F1 (N=2) and F2 (N=4) families under common garden conditions and used these fish
65 for genome-wide linkage map construction (Table S1) and quantitative trait loci (QTL) mapping.
66 Using 25,001 high-quality single nucleotide variants generated from restriction site-associated

67 DNA (RAD) sequencing, we identified one significant QTL for each thermal tolerance trait (Fig.
68 2b) that explained a high percentage of trait variance (PVE; CTmin = 54%, CTmax = 64%).
69 We used these genetically based traits to inform the boundaries of three distinct
70 environmental regions in species distribution models (SDMs) for marine stickleback based on
71 varying levels of physiological performance: i) a 'normal behaviour' envelope with
72 environmental temperatures associated with an absence of an observable behavioural stress
73 response (5.0 to 25.0 °C), ii) a 'within physiological limits' envelope with environmental
74 temperatures that fall within the range of the measured physiological limits (0.85 to 31.9 °C) ,
75 and iii) an 'outside of physiological limits' envelope with environmental temperatures that fall
76 outside the measured physiological limits (below 0.85 and above 31.9 °C). Based on sea ice
77 extent and bathymetry alone, our present-day correlative SDM suggests a marine range
78 distribution for these stickleback from the southern Bering Sea to northern Washington state, and
79 along the southeast Alaskan Panhandle (combined shaded area in Fig. 3a). When we include
80 species-specific thermal trait data from the wild marine populations, nearly the entire range of
81 suitable habitat was unaffected by thermal tolerance limits, with the exception of a slight
82 restriction at the northern end of the range (Fig. 3a). However, when restricted to the Normal
83 Behaviour area, the range becomes confined to the west of the northern tip of Kodiak Island (Fig.
84 3a), a limit coinciding with the northern-most known marine population in the Pacific Northwest
85 genetic cluster[19].
86 We next generated SDMs based on predicted end-of-century environmental variables
87 according to the Intergovernmental Panel on Climate Change (IPCC) representative
88 concentration pathways (RCPs) 4.5 and 8.5 from the Fifth Assessment Report[14,20]. End-of-
89 century IPCC predictions resulted in a substantial increase in the overall suitable habitat area for

stickleback, with a 2.25-fold or 1,338,219 $km^2$ increase (combined shaded area in Fig. 3b-e) in association with a reduction in sea ice concentration at the northern end of the range. When temperature increases as predicted by RCP 4.5 in the 'no evolution' model, there is a 5.86-fold (1,011,949 $km^2$) increase in the Normal Behaviour area within this newly suitable habitat (Fig. 3b) when compared to the current day model. Under RCP 8.5 in the 'no evolution' model, the entirety of suitable habitat area remains within tolerable limits (Fig. 3c), with a smaller proportion of the range falling outside of the Normal Behaviour area compared to RCP 4.5 (10.7%) 'no evolution' model.

Incorporating the evolution of CTmin into the SDMs ('evolution' model) results in a large increase in the proportion of suitable habitat that falls within the Normal Behaviour area. We allowed CTmin to evolve at a rate of 0.63 *haldanes*, which is equal to the rate observed for CTmin in marine stickleback[4] (there are currently no empirical estimates of evolutionary rate for CTmax). Under RCP 4.5, almost all (99.9%) of the suitable habitat range falls within the Normal Behaviour area (Fig. 3d), while under the RCP 8.5 'evolution' model, the entire range of suitable habitat is within the Normal Behaviour area (Fig. 3e). These represent a 7.45-fold increase (1,336,123 $km^2$) for RCP 4.5 and 7.46-fold increase (1,338,219 $km^2$) for RCP 8.5 in the Normal Behaviour area when compared to the current day SDM.

We next considered the effect of limiting the evolutionary rate of CTmin based on the observed genetic architecture of a single major effect locus ('PVE' model). Under the RCP 4.5 'PVE' model, we observed a 1.08-fold reduction in the Normal Behaviour area (109,120 $km^2$, Fig. S3) when compared to the 'evolution' model (Fig. 3d). Under RCP 8.5 projections with the 'PVE' model, we observed a 3,905 $km^2$ decrease in the Normal Behaviour area (Fig. S3) when compared to the 'evolution' model (Fig. 3e). This relatively small reduction in Normal

113 Behaviour area with adjusted PVE for the thermal traits under RCP 8.5 still results in a
114 1,334,314 $km^2$ increase in area compared to the current day SDM.

115 **Discussion**

116 We assessed the critical thermal minimum (CTmin) and maximum (CTmax) for
117 threespine stickleback from wild marine and freshwater populations, as well as F1 and F2
118 families in order to determine the genetic basis underlying traits that will be important for
119 population persistence under climate change. We incorporated the empirical ecological and
120 evolutionary trait data from wild marine populations into mechanistic species distribution models
121 under two climate change scenarios. We estimated the species distribution in the Pacific
122 Northwest marine environment while these traits were held constant ('no evolution'), allowed
123 CTmin to evolve in accordance with evolutionary rate estimates ('evolution'), and allowed
124 CTmin to evolve at a constrained rate associated with the percent of trait variance explained by
125 the single QTL we detected ('PVE'). The geographic ranges predicted for the end-of-century
126 species distributions increased by over 7-fold (RCP 4.5: 1,336,123 $km^2$; RCP 8.5: 1,338,219
127 $km^2$) when CTmin was allowed to evolve, a substantial increase over the 'no evolution' model.
128 Additionally, when CTmin evolution was constrained in the PVE model, there remained a ~6-
129 fold increase (RCP 4.5: 1,227,002 $km^2$; RCP 8.5: 1,334,314 $km^2$) in the geographic range
130 compared to current day. These differences in the predicted distributions underline the
131 significance of incorporating empirical evolutionary data into SDMs[5,21,22], and in particular the
132 need to consider behaviour in addition to physiology when predicting range shifts[23].

133 While the results presented here showcase the importance of creating more robust and
134 informed SDMs, they also highlight a number of aspects that will benefit from additional
135 consideration when interpreting these models. The existing estimate of CTmin evolution in

136 sticklebacks considered the change in phenotypic variation across generations[4], rather than
137 evolution at underlying loci. As such, it is likely that some proportion of the observed phenotypic
138 change was due to plastic responses. In our PVE model, we take a conservative approach by
139 restricting phenotypic evolution of CTmin to only occur through heritable change via the locus
140 shown to be associated with the trait. The efficiency of translating the selection acting on a trait
141 into evolutionary response across generations can depend on the genetic architecture of the
142 trait[24]. The large effect loci that we identified here are consistent with expectations from theory
143 suggesting that prolonged bouts of adaptation with gene flow (as expected in this system[24–26])
144 should favour architectures characterized by fewer, larger effect, more tightly linked alleles[27–29].
145 However, it should be noted that the effects of the two QTL identified here are likely
146 overestimated and other loci might have gone undetected (*sensu* the Beavis Effect[30]). The joint
147 action of plastic effects and evolution at undetected loci might therefore result in range
148 distributions that are more similar to those predicted in our 'evolution' models.

149 Climate change is leading to an increase in the frequency of extreme temperature
150 events[14,31], including both extreme heat and extreme cold[32–34], which could drive selection on
151 both CTmin and CTmax[13,35–37]. Our models reveal that the evolution of cold tolerance can have a
152 significant impact on predicted range distributions despite most end-of-century climate change
153 scenarios involving an overall warmer, not cooler world. This counterintuitive result occurs
154 because climate change opens up newly available thermal niche space in waters north of the
155 current day geographic range[20], and the evolution of CTmin extends this range expansion further
156 still. Northward range expansion with climate change due to increasing habitat availability has
157 also been documented in birds[38–41], plants[42], other fishes[43–45], and pest species (such as ticks[46–48]
158 and mountain pine beetle[49,50]), as well as in large scale analyses of diverse taxa assessing the

159 ‘fingerprints’ of climate change impacts[51,52]. However, it is likely that evolution of CTmax will
160 also play a role in responses to environmental change[53–55]. Although we have no empirical
161 estimates of CTmax evolution, it is interesting to explore how distributions would shift if we
162 observed the same rate of evolution in this trait as in CTmin. Using the same rate of haldanes and
163 incorporating our observed PVE for the locus associated with CTmax, we find that geographic
164 ranges predicted for the end-of-century species distributions also increased by over 7-fold (RCP
165 4.5: 1,227,002 $km^2$ increase; RCP 8.5: 1,334,314 $km^2$ increase; Fig. S4). Further investigations to
166 test the empirical rate of evolution of thermal behaviour, physiology and the molecular
167 underpinnings of these key traits would be well served by assessing additional samples along the
168 latitudinal gradient inhabited by stickleback to gain a more detailed understanding of these
169 temperature-associated traits over a wider environmental range.

170 Collectively, the inclusion of thermal traits and their evolution alters the projected ranges
171 of threespine stickleback, with a substantial increase in the predicted area that the species will
172 occupy under climate change forecasts. Many traits are evolving in response to climate change[56–
173 59] and SDMs that do not take trait data (and trait evolution) into account could provide inaccurate
174 predictions about future species distributions under climate change[3] - an issue of particular
175 concern for species at risk and pest species undergoing range expansion[60–62]. Our results provide
176 a framework for addressing this problem, which will have critical implications for the application
177 of these models in policy and resource management, and the protection of biodiversity in a
178 changing climate.

## Materials and Methods

Sample collection and husbandry

We collected adult *Gasterosteus aculeatus* (Fig. 1a) from two marine populations (Bamfield, M1, 48°49'12.69"N 125° 8'57.90"W; Garden Bay Lagoon, M2, 49°37'52.84"N 124° 1'49.26"W) and two freshwater populations (Hotel Lake, FW1, 49°38'26.94"N 124° 3'0.69"W; Klein Lake, FW2, 49°43'32.47"N 123°58'7.83"W) in southwestern British Columbia (Fig. 1b). Individuals were maintained in a flow-through system and photoperiod that mimicked the source populations during collection periods before transport. We transported the fish to our aquatics facility in the Life and Environmental Sciences Animal Resources Centre at the University of Calgary, where we separated the fish into population-specific 113 L glass aquaria at a density of approximately 20 fish per aquarium. We acclimated marine individuals to freshwater salinity over one week and maintained fish in a common environment (salinity of 4-6 ppt, water temperature of 15 ± 2 °C, and a photoperiod of 16L:8D). Individuals were allowed to acclimate for at least 2 weeks before experiments (1 week for stress reduction post-transfer, 1 week for common garden environment acclimation and salinity ramp). Each common garden aquarium was on a closed system with individual filters, air stones, and water supply. We fed all adult fish *ad libitum* once per day with thawed bloodworms (Hikari Bio-Pure Frozen Bloodworms). All collections and transfers were approved by the Department of Fisheries and Oceans (marine collections and transfers), the Ministry of Forests, Lands, and Natural Resource Operations (freshwater collections), and the Huu-ay-aht First Nations (marine collections).

Crossing design for marine and freshwater F1 families

We collected eggs from females and fertilized the eggs with extracted testes from euthanized males. We transferred the fertilized egg mass to a mesh-bottomed egg incubator

202 suspended in a 37 L aquarium for hatching. Each hatching aquarium was maintained with a
203 single air stone and a filter. Once hatched, we reared the larval fish in 37 L hatching aquaria until
204 they reached a total length (TL) of approximately 1 cm, after which we split the families into
205 family-specific 113 L aquaria to maintain suitable densities. We fed the larval fish *ad libitum*
206 twice daily with live *Artemia spp.* nauplii, and then gradually transitioned the diet to chopped,
207 thawed bloodworms (Hikari Bio-Pure Frozen Bloodworms) *ad libitum* once daily as they
208 reached approximately 2 cm TL. The F1 families were maintained in a common garden
209 environment identical to that of the F0 populations. We produced one F1 family for each
210 population (M1_F1, M2_F2, FW1_F1, and FW2_F1).

211 Crossing design for hybrid mapping families

212 To generate genetically heterogeneous marine-freshwater F1 families from wild F0
213 parents, we collected eggs from marine females and fertilized the eggs with extracted testes from
214 euthanized freshwater males. Egg masses were hatched, and juveniles were reared, as detailed
215 above. Overall, we produced one F1 family of M1xFW1 hybrids (hereafter referred to as H1_F1)
216 and three F1 families of M1xFW2 hybrids (hereafter referred to as H2_F1). The hybrid F1
217 families were maintained in a common garden environment identical to that of the F0
218 populations. To generate F2 families for linkage map construction, we crossed individuals from
219 the same F1 family with the same methodology used to generate the F1 families. Overall, we
220 produced one F2 family of H1xH1 hybrids (referred to as H1_F2) and three families of H2xH2
221 hybrids (referred to as H2_F2_1, H2_F2_2, and H2_F2_3). All F2 individuals were raised as
222 described above in a common garden environment identical to that of the F0 and F1 individuals
223 to ensure consistent history and use for QTL mapping.

224 Thermal tolerance experiments

225 To assess the lower and upper limits of physiological thermal tolerance, we conducted
226 standard critical thermal minimum (CTmin) and maximum (CTmax) experiments on adult
227 fish[4,63,64]. At these sublethal limits, the fish experiences a loss of equilibrium (LOE) at which
228 they lose the ability to escape conditions that would ultimately lead to their death in nature[65]. Our
229 experimental tank held 1000 mL glass beakers aerated individually to prevent thermal
230 stratification. Before each experiment, individuals were fasted for 24 hours. After a 15-minute
231 acclimation to the experimental apparatus in the individual beakers, we cooled or heated the
232 water (for CTmin or CTmax, respectively) at a rate of approximately 0.33 °C $min^{-1}$. We assessed
233 wild F0 individuals ($n_{M1}$ = 32, $n_{M2}$ = 14, $n_{FW1}$ = 15, $n_{FW2}$ = 16, $N$ = 77; Fig. 1c) and lab raised F1
234 ($n_{M1_F1}$ = 13, $n_{M2_F1}$ = 15, $n_{FW1_F1}$ = 15, $n_{FW2_F1}$ = 15, $N$ = 58; Fig. S1) and F2 individuals ($n_{H1_F2}$
235 = 28, $n_{H2_F2_1}$ = 36, $n_{H2_F2_2}$ = 21, $n_{H2_F2_3}$ = 17, $N$ = 102; Fig. S2). All individuals were
236 assessed for CTmin, allowed to recover for at least three days, then assessed for CTmax to keep
237 thermal stress history consistent. The onset of erratic behaviours associated with a behavioural
238 stress response occurred below 5.0 °C and above 25.0 °C during CTmin and CTmax
239 experiments, respectively. Normal behaviour was observed between 5.0 °C and 25.0 °C, whereas
240 outside of those temperatures, individuals gradually exhibited more extreme stress responses
241 (*e.g.,* increased gilling rate, erratic movement, muscle spasms, listing, as outlined by the
242 Canadian Council of Animal Care guidelines) until reaching LOE and the inability of an
243 individual to right itself (the experimental endpoint)[4,63,64]. At the time of data collection for
244 thermal trait experiments, all individuals were adults.

245 Isolation and characterization of single nucleotide polymorphisms (SNPs)

246 Genomic DNA was extracted from caudal fin tissue using a phenol-chloroform-based
247 protocol. We digested tissues overnight in digestion buffer and proteinase K at 55 °C, then
248 performed multiple phenol-chloroform and ethanol washes to isolate the DNA. We assessed the
249 quantity of the extracted DNA using the Quant-iT PicoGreen dsDNA assay kit (ThermoFisher
250 Scientific, Waltham, MA, USA) and Synergy HT plate reader with the Gen5 associated software
251 (BioTek, Winooski, VT, USA). We prepared restriction site-associated DNA (RAD)
252 libraries(Peterson et al. 2012) using *MluCl* and *NlaIII* restriction (New England Biolabs,
253 Ipswich, MA, USA), ligation of individual barcodes, and pooling of 48 individuals per library at
254 equimolar concentrations. We performed a final PCR to amplify DNA and add library-specific
255 indices to allow for pooling of multiple libraries. We sequenced three libraries at McGill
256 University and Génome Québec Innovation Center on one lane of Illumina HiSeq 4000 (Illumina
257 Inc., San Diego, CA, USA).

258 Assembly of genetic linkage map

259 After barcode demultiplexing and filtering out low quality reads in STACKS[66], we
260 removed PCR duplicates from the raw sequences and aligned to the *G. aculeatus* reference
261 genome[17] using the Burrows-Wheeler transform[67]. Individual libraries were concatenated and
262 filtered[68] using *vcftools* v3.0[69] and then split into chromosome-specific VCF files to assemble the
263 linkage maps chromosome by chromosome. We assigned markers to a linkage group with an
264 initial LOD score of 3 after filtering out markers that showed high levels of segregation
265 distortion and missing observations (> 20% missing data) in Lep-MAP3[70]. Unassigned markers
266 were subsequently added to the existing linkage group at a LOD score of 3 and a size limit of 5
267 markers per linkage group. We ordered the markers using a minimum posterior value of 0.001

268 and collapsed multiple markers when the probability difference between markers was < 0.01[70].
269 The final linkage map was subset for use in R[71] with a custom Python script to visualize the
270 linkage map and to generate a list of informative SNPs to use in subsequent analyses with the *qtl*
271 v1.44-9[72] and *qtlTools* v1.2.0[73] packages. Linkage maps were visualized using
272 *LinkageMapView*[74] in R[71]. The final linkage maps were similar across families in number of
273 markers, length, and spacing between markers, though the H1_F2 map did have a higher density
274 of markers (Table S1).

275 Quantitative trait loci (QTL) mapping

276 We analysed families separately with the same methodology to assess the presence of
277 QTL associated with the thermal traits. We calculated conditional genotype probabilities using
278 hidden Markov model technology and simulated genotypes based on the observed marker data
279 (allowing for possible genotyping errors at a level of 0.0001 using a Kosambi mapping function
280 with a fixed step width) prior to running genome scans with a single QTL model[75,76]. We
281 determined the logarithm of the odds (LOD) score significance thresholds for each trait through
282 permutation tests for each family (100,000 permutations) (Fig. 2a). We pulled significant QTL
283 above the genome-wide significance threshold ($\alpha = 0.05$[77]), calculated confidence intervals of
284 QTL location based on nearby markers, and estimated the percent variance explained by each
285 QTL peak marker. We identified two QTL on linkage group 4 (which corresponds to
286 chromosome 4 of the BROAD assembly[17]) associated with CTmin and CTmax (Fig. 2b).

287 Environmental variables and species distribution models (SDMs)

288 We compiled environmental data widely used in the construction of SDMs to estimate
289 suitable habitat in both present day and end-of-century forecasts[78], including bathymetry, sea ice
290 extent and concentration, salinity, and sea surface temperature. We used 2014 data as our

291 baseline year to match the forecasting baseline of the Fifth Assessment Report[14]. We assumed a
292 suitable habitat range for this species in the Pacific Northwest to consist of coastal areas (where
293 the water depth is less than 200 m) where sea ice is never present (*i.e.,* no sea ice at the
294 maximum extent). The salinity tolerance for *G. aculeatus* is very wide[79,80] and salinity was not
295 limiting in any of the habitat[81], therefore salinity was not included in the final present day or
296 forecasted models. We obtained bathymetry data from the General Bathymetric Chart of the
297 Oceans (GEBCO) of the British Oceanographic Data Centre[82], and maximum sea ice extent data
298 from the Multisensory Analyzed Sea Ice Extent – Northern Hemisphere (MASIE-NH) product[83].
299 We obtained maximum and minimum daily mean sea surface temperature (SST)[84]. Sea surface
300 temperature was used as a proxy for water temperature. Stickleback thermal trait data were used
301 to set the limits of the distribution within the possible area delineated by sea ice free water of a
302 suitable depth (Table S2). The thermal trait measurements were all based on our experimental
303 findings reported here.
304 In the end-of-century forecast for suitable habitat, we assumed bathymetry to be
305 consistent with the modern scenario. However, the Arctic Ocean is predicted to be
306 predominantly free of sea ice in the summer by the end of the century[85], with significant end-of-
307 century reductions in winter/spring sea ice concentration (reduced to a concentration of 0.1 at the
308 Seward Peninsula[85]), so we conservatively set the maximum northern extent of the suitable
309 habitat to be 65°35' N, which corresponds to the western tip of the Seward Peninsula (near
310 Wales, AK). The extent of sea ice was kept consistent between scenarios to control for area in
311 calculations of range expansion. The water temperatures were increased based on projections for
312 large marine ecosystems of Northern Oceans from global climate models[14,20]. Maps were created
313 in R[71] using the packages *raster* v. 3.3-13[86] and *rgeos* v. 0.5-3[87].

We incorporated the experimental data from the critical thermal minimum and maximum trials on the wild marine populations (Fig. 1c) to understand how trait inclusion may affect range projections under climate change. These trait-defined envelopes were overlain on the suitable habitat background to delineate projected presence based on thermal traits in both current day and IPCC predicted RCPs 4.5 and 8.5. The trait values were kept constant (*i.e.,* not changed) in the 'no evolution' projections, but in the 'evolution' projections, we allowed CTmin to evolve an improvement of 2.5 °C (*i.e.,* 2.5 °C lower than CTmin boundary in the 'no evolution' projection) by the end of the century based on a rate of 0.63 *haldanes* from a selection experiment previously conducted on populations from this same genetic cluster[4]. The 'evolution' model assumes whole-organism tolerance evolution with selection acting on 100% of the loci affecting CTmin evolution. Therefore, to account for the observed genetic architecture of a single, large effect locus associated with CTmin, we next considered a 'PVE' model, where CTmin was allowed to evolve to only 54% of the total estimated trait value from the 'evolution' model (*i.e.,* 2.5 °C * 0.54). However, a notable restriction in the evolution of CTmin for both models ('evolution' and 'PVE') was a hard boundary drawn at 0 °C under the assumption that population persistence in a sub-zero environment would require many additional adaptations alongside CTmin improvement (*e.g.,* extreme adaptations observed in Antarctic notothenioid fishes[88–90]).

To quantify the differences in estimated suitable habitat under current day and end-of-century conditions, we compared areas for each warming scenario to the equivalent scenario under current conditions. Similarly, to compare the differences in evolutionary scenarios, the area of each end-of-century evolutionary trajectory was compared to either the contrasting RCP projection or adjusted PVE projection. For these comparisons, we used North Pole Lambert

337 azimuthal equal area projection for all maps, and georeferenced to known landmarks in ArcGIS
338 v10.8[91] to calculate area from the maps generate in R[71] (conversion ratio of 7873.42).
339 The datasets generated and analysed during the current study are available from the
340 corresponding author upon reasonable request. The annotated code, including all parameter
341 thresholds, for the above QTL analyses and SDM construction is publicly available on Github
342 (github.com/sjswuitchik/gasAcu_qtl_sdm).
343

344 **References**


345 1. Kearney, M. R., Wintle, B. A. & Porter, W. P. Correlative and mechanistic models of
346 species distribution provide congruent forecasts under climate change. *Conserv. Lett.* **3**,
347 203–213 (2010).

348 2. Kearney, M. & Porter, W. Mechanistic niche modelling: Combining physiological and
349 spatial data to predict species' ranges. *Ecol. Lett.* **12**, 334–350 (2009).

350 3. Bush, A. *et al.* Incorporating evolutionary adaptation in species distribution modelling
351 reduces projected vulnerability to climate change. *Ecol. Lett.* **19**, 1468–1478 (2016).

352 4. Barrett, R. D. H. *et al.* Rapid evolution of cold tolerance in stickleback. *Proc. R. Soc. B*
353 **278**, 233–238 (2011).

354 5. Evans, T. G., Diamond, S. E. & Kelly, M. W. Mechanistic species distribution modelling
355 as a link between physiology and conservation. *Conserv. Physiol.* **3**, 1–16 (2015).

356 6. Pearce, J. & Lindenmayer, D. Bioclimatic analysis to enhance reintroduction biology of
357 the endangered helmeted honeyeater (Lichenostomus melanops cassidix) in southeastern

358 Australia. *Restor. Ecol.* **6**, 238–243 (1998).

359 7. Araújo, M. B., Cabeza, M., Thuiller, W., Hannah, L. & Williams, P. H. Would climate
360 change drive species out of reserves? An assessment of existing reserve-selection
361 methods. *Glob. Chang. Biol.* **10**, 1618–1626 (2004).

362 8. Hochachka, P. W. & Somero, G. N. Mechanism and process in physiological evolution.
363 *Biochem. Adapt.* **480**, (2002).

364 9. Huey, R. B. & Slatkin, M. Costs and benefits of lizard thermoregulation. *Q. Rev. Biol.* **51**,
365 363–384 (1976).

366 10. Coutant, C. C. Thermal preference: when does an asset become a liability? *Environ. Biol.*
367 *Fishes* **18**, 161–172 (1987).

368 11. Huey, R. B. & Kingsolver, J. G. Evolution of thermal sensitivity of ectotherm
369 performance. *Trends Ecol. Evol.* **4**, 131–135 (1989).

370 12. Sexton, J. P., McIntyre, P. J., Angert, A. L. & Rice, K. J. Evolution and Ecology of
371 Species Range Limits. *Annu. Rev. Ecol. Evol. Syst.* **40**, 415–436 (2009).

372 13. Hoffman, A. & Sgrò, C. Climate change and evolutionary adaptation. *Nature* **470**, 479–
373 485 (2011).

374 14. IPCC. *Climate Change 2014: Synthesis Report*. *Fifth Assessment Report of the*
375 *Intergovernmental Panel on Climate Change* (2014). doi:10.1016/S0022-0248(00)00575-
376 3

377 15. Eyer, P. A., Blumenfeld, A. J. & Vargo, E. L. Sexually antagonistic selection promotes

genetic divergence between males and females in an ant. *Proc. Natl. Acad. Sci. U. S. A.* **116**, 24157–24163 (2019).

16. Hendry, A. P., Peichel, C. L., Matthews, B., Boughman, J. W. & Nosil, P. Stickleback research: The now and the next. *Evol. Ecol. Res.* **15**, 111–141 (2013).

17. Jones, F. C. *et al.* The genomic basis of adaptive evolution in threespine sticklebacks. *Nature* **484**, 55–61 (2012).

18. Barrett, R. D. H. & Hendry, A. P. Evolutionary rescue under environmental change. in *Behavioural responses to a changing world: mechanisms and consequences* 216–233 (Oxford University Press Oxford, UK, 2012).

19. Morris, M. R. J., Bowles, E., Allen, B. E., Jamniczky, H. A. & Rogers, S. M. Contemporary ancestor? Adaptive divergence from standing genetic variation in Pacific marine threespine stickleback. *BMC Evol. Biol.* **18**, 1–21 (2018).

20. Alexander, M. A. *et al.* Projected sea surface temperatures over the 21st century: Changes in the mean, variability and extremes for large marine ecosystem regions of Northern Oceans. *Elementa* **6**, (2018).

21. Buckley, L. *et al.* Can mechanism inform species' distribution models? *Ecol. Lett.* **13**, 1041–1054 (2010).

22. Lyon, N. J., Debinski, D. M. & Rangwala, I. Evaluating the Utility of Species Distribution Models in Informing Climate Change-Resilient Grassland Restoration Strategy. *Front. Ecol. Evol.* **7**, 1–8 (2019).

398 23. Sunday, J. M., Bates, A. E. & Dulvy, N. K. Thermal tolerance and the global
399 redistribution of animals. *Nat. Clim. Chang.* **2**, 686–690 (2012).

400 24. Rogers, S. M. *et al.* Genetic Signature of Adaptive Peak Shift in Threespine Stickleback.
401 *Evolution (N. Y).* 2439–2451 (2012). doi:10.5061/dryad.6jj614kh

402 25. Schluter, D., Marchinko, K. B., Barrett, R. D. H. & Rogers, S. M. Natural selection and
403 the genetics of adaptation in threespine stickleback. *Philos. Trans. R. Soc. B Biol. Sci.* **365**,
404 2479–2486 (2010).

405 26. Jones, F. C. *et al.* A genome-wide SNP genotyping array reveals patterns of global and
406 repeated species-pair divergence in sticklebacks. *Curr. Biol.* **22**, 83–90 (2012).

407 27. Yeaman, S. & Otto, S. P. Establishment and maintenance of adaptive genetic divergence
408 under migration, selection, and drift. *Evolution (N. Y).* **65**, 2123–2129 (2011).

409 28. Yeaman, S. & Whitlock, M. C. The genetic architecture of adaptation under migration-
410 selection balance. *Evolution (N. Y).* **65**, 1897–1911 (2011).

411 29. Via, S., Conte, G., Mason-Foley, C. & Mills, K. Localizing FST outliers on a QTL map
412 reveals evidence for large genomic regions of reduced gene exchange during speciation-
413 with-gene-flow. *Mol. Ecol.* **21**, 5546–5560 (2012).

414 30. Beavis, W. The power and deceit of QTL experiments: lessons from comparative QTL
415 studies. in *49th Annual Corn & Sorghum Research Conference* 250–266 (1994).

416 31. Stott, P. How climate change affects extreme weather events. *Science (80-. ).* **352**, 1517–
417 1518 (2016).

418 32. Herring, S., Hoerling, M., Kossing, J., Peterson, T. & Stott, P. Explaining extreme events
419 of 2014 from a climate perspective. **96**, 1–180 (2015).

420 33. Herring, S. C. *et al.* Explaining extreme events of 2016 from a climate perspective. *Bull.*
421 *Am. Meteorol. Soc.* **99**, S1–S157 (2018).

422 34. Herring, S. C., Christidis, N., Hoell, A., Hoerling, M. P. & Stott, P. Explaining extreme
423 events of 2018 from a climate perspective. *Bull. Am. Meteorol. Soc.* **101**, 1–146 (2020).

424 35. Kingsolver, J. G. *et al.* Complex life cycles and the responses of insects to climate change.
425 *Integr. Comp. Biol.* **51**, 719–732 (2011).

426 36. Denny, M. W. & Dowd, W. W. Biophysics, environmental stochasticity, and the evolution
427 of thermal safety margins in intertidal limpets. *J. Exp. Biol.* **215**, 934–947 (2012).

428 37. Buckley, L. B. & Huey, R. B. How extreme temperatures impact organisms and the
429 evolution of their thermal tolerance. *Integr. Comp. Biol.* **56**, 98–109 (2016).

430 38. Tingley, M. W., Monahan, W. B., Beissinger, S. R. & Moritz, C. Birds track their
431 Grinnellian niche through a century of climate change. *Proc. Natl. Acad. Sci. U. S. A.* **106**,
432 19637–19643 (2009).

433 39. Melles, S. J., Fortin, M. J., Lindsay, K. & Badzinski, D. Expanding northward: Influence
434 of climate change, forest connectivity, and population processes on a threatened species'
435 range shift. *Glob. Chang. Biol.* **17**, 17–31 (2011).

436 40. Tombre, I. M., Oudman, T., Shimmings, P., Griffin, L. & Prop, J. Northward range
437 expansion in spring-staging barnacle geese is a response to climate change and population

growth, mediated by individual experience. *Glob. Chang. Biol.* **25**, 3680–3693 (2019).

41. Rushing, C. S., Andrew Royle, J., Ziolkowski, D. J. & Pardieck, K. L. Migratory behavior and winter geography drive differential range shifts of eastern birds in response to recent climate change. *Proc. Natl. Acad. Sci. U. S. A.* **117**, 12897–12903 (2020).

42. D'Andrea, L. *et al.* Climate change, anthropogenic disturbance and the northward range expansion of Lactuca serriola (Asteraceae). *J. Biogeogr.* **36**, 1573–1587 (2009).

43. Fossheim, M. *et al.* Recent warming leads to a rapid borealization of fish communities in the Arctic. *Nat. Clim. Chang.* **5**, 673–677 (2015).

44. Yapıcı, S., Bilge, G. & Filiz, H. Northwards range expansion of Sparisoma cretense (Linnaeus, 1758) in the Turkish Aegean Sea. *J. Aquac. Eng. Fish. Res.* 201–207 (2016). doi:10.3153/jaefr16022

45. Spies, I. *et al.* Genetic evidence of a northward range expansion in the eastern Bering Sea stock of Pacific cod. *Evol. Appl.* **13**, 362–375 (2020).

46. Ogden, N. H. *et al.* Climate change and the potential for range expansion of the Lyme disease vector Ixodes scapularis in Canada. *Int. J. Parasitol.* **36**, 63–70 (2006).

47. Clow, K. M. *et al.* Northward range expansion of Ixodes scapularis evident over a short timescale in Ontario, Canada. *PLoS One* **12**, 1–15 (2017).

48. Sagurova, I. *et al.* Predicted northward expansion of the geographic range of the tick vector amblyomma americanum in North America under future climate conditions. *Environ. Health Perspect.* **127**, 1–14 (2019).

458 49. Kurz, W. A. *et al.* Mountain pine beetle and forest carbon feedback to climate change.
459 *Nature* **452**, 987–990 (2008).

460 50. Sambaraju, K. R., Carroll, A. L. & Aukema, B. H. Multiyear weather anomalies
461 associated with range shifts by the mountain pine beetle preceding large epidemics. *For.*
462 *Ecol. Manage.* **438**, 86–95 (2019).

463 51. Parmesan, C. & Yohe, G. A globally coherent fingerprint of climate change impacts
464 across natural systems. **421**, 37–42 (2003).

465 52. Platts, P. J. *et al.* Habitat availability explains variation in climate-driven range shifts
466 across multiple taxonomic groups. *Sci. Rep.* **9**, 1–10 (2019).

467 53. Geerts, A. N. *et al.* Rapid evolution of thermal tolerance in the water flea Daphnia. *Nat.*
468 *Clim. Chang.* **5**, 665–668 (2015).

469 54. Bozinovic, F., Medina, N. R., Alruiz, J. M., Cavieres, G. & Sabat, P. Thermal tolerance
470 and survival responses to scenarios of experimental climatic change: changing thermal
471 variability reduces the heat and cold tolerance in a fly. *J. Comp. Physiol. B Biochem. Syst.*
472 *Environ. Physiol.* **186**, 581–587 (2016).

473 55. Cuenca Cambronero, M., Beasley, J., Kissane, S. & Orsini, L. Evolution of thermal
474 tolerance in multifarious environments. *Mol. Ecol.* **27**, 4529–4541 (2018).

475 56. Eliason, E. J. *et al.* Differences in thermal tolerance among sockeye salmon populations.
476 *Science (80-. ).* **332**, 109–112 (2011).

477 57. Hovel, R. A., Carlson, S. M. & Quinn, T. P. Climate change alters the reproductive

478 phenology and investment of a lacustrine fish, the three-spine stickleback. *Glob. Chang.*
479 *Biol.* 1–13 (2016). doi:10.1111/gcb.13531

480 58. Gómez-Ruiz, E. P. & Lacher, T. E. Climate change, range shifts, and the disruption of a
481 pollinator-plant complex. *Sci. Rep.* **9**, 1–10 (2019).

482 59. Horton, K. G. *et al.* Phenology of nocturnal avian migration has shifted at the continental
483 scale. *Nat. Clim. Chang.* **10**, 63–68 (2020).

484 60. Cullingham, C. I. *et al.* Mountain pine beetle host-range expansion threatens the boreal
485 forest. *Mol. Ecol.* **20**, 2157–2171 (2011).

486 61. McLeod, D. J., Hallegraeff, G. M., Hosie, G. W. & Richardson, A. J. Climate-driven
487 range expansion of the red-tide dinoflagellate Noctiluca scintillans into the Southern
488 Ocean. *J. Plankton Res.* **34**, 332–337 (2012).

489 62. Bebber, D. P. Range-Expanding Pests and Pathogens in a Warming World. *Annu. Rev.*
490 *Phytopathol.* **53**, 335–356 (2015).

491 63. Hutchison, V. H. Comparative Biology Critical Thermal Maxima in Salamanders. *Physiol.*
492 *Zool.* **34**, 92–125 (1961).

493 64. Fangue, N. A., Hofmeister, M. & Schulte, P. M. Intraspecific variation in thermal
494 tolerance and heat shock protein gene expression in common killifish, Fundulus
495 heteroclitus. *J. Exp. Biol.* **209**, 2859–2872 (2006).

496 65. Beitinger, T., Bennett, W. & McCauley, R. Temperature tolerances of North American
497 freshwater fishes exposed to dynamic changes in temperature. *Environ. Biol. Fishes* **58**,

498 237–275 (2000).

499 66. Catchen, J., Hohenlohe, P. A., Bassham, S., Amores, A. & Cresko, W. A. Stacks: An
500 analysis tool set for population genomics. *Mol. Ecol.* **22**, 3124–3140 (2013).

501 67. Li, H. & Durbin, R. Fast and accurate long-read alignment with Burrows-Wheeler
502 transform. *Bioinformatics* **26**, 589–595 (2010).

503 68. Puritz, J. B., Hollenbeck, C. M. & Gold, J. R. *dDocent* : a RADseq, variant-calling
504 pipeline designed for population genomics of non-model organisms. *PeerJ* **2**, e431 (2014).

505 69. Danecek, P. *et al.* The variant call format and VCFtools. *Bioinformatics* **27**, 2156–2158
506 (2011).

507 70. Rastas, P. Lep-MAP3: Robust linkage mapping even for low-coverage whole genome
508 sequencing data. *Bioinformatics* **33**, 3726–3732 (2017).

509 71. R Core Team. R: A language and environment for statistical computing. (2019).

510 72. Broman, K. W., Wu, H., Sen, Ś. & Churchill, G. A. R/qtl: QTL mapping in experimental
511 crosses. *Bioinformatics* **19**, 889–890 (2003).

512 73. Lovell, J. qtlTools. (2019).

513 74. Ouellette, L. A., Reid, R. W., Blanchard, S. G. & Brouwer, C. R. LinkageMapView-
514 rendering high-resolution linkage and QTL maps. *Bioinformatics* **34**, 306–307 (2018).

515 75. Broman, K. W. & Sen, S. *A Guide to QTL Mapping with R/qtl*. **46**, (Springer, 2009).

516 76. Arends, D., Prins, P., Broman, K. W. & Jansen, R. C. *Tutorial-Multiple-QTL Mapping*

*(MQM) Analysis for R/qtl*. *http://www.rqtl.org/tutorials/MQM-tour.pdf* (2014).

77. Greenwood, A. K. *et al.* The genetic basis of divergent pigment patterns in juvenile threespine sticklebacks. *Heredity (Edinb).* **107**, 155–166 (2011).

78. Wiens, J., Stralberg, D., Jongsomjit, D., Howell, C. & Snyder, M. Niches, models, and climate change: Assessing the assumptions and uncertainties. *Proc. Natl. Acad. Sci.* **106**, 19729–19736 (2009).

79. Bayly, I. A. E. Salinity Tolerance and Osmotic Behavior of Animals in Athalassic Saline and Marine Hypersaline Waters. *Annu. Rev. Ecol. Syst.* **3**, 233–268 (2003).

80. Divino, J. N. *et al.* Osmoregulatory physiology and rapid evolution of salinity tolerance in threespine stickleback recently introduced to fresh water. *Evol. Ecol. Res.* **17**, 179–201 (2016).

81. Zweng, M. M. *et al. World Ocean Atlas 2013, Volume 2: Salinity*. *NOAA Atlas NESDIS 74* **2**, (2013).

82. Weatherall, P. *et al.* A new digital bathymetric model of the world's oceans. *Earth Sp. Sci.* **2**, 331–345 (2015).

83. Fetterer, F., Savoie, M., Helfrich, S. & Clemene-Colon, P. U.S. National Ice Center and National Snow and Ice Data Center. *Multisensor Analyzed Sea Ice Extent - Northern Hemisphere (MASIE-NH)* (2010). doi:https://doi.org/10.7265/N5GT5K3K.

84. Reynolds, R. *et al.* Daily High-Resolution-Blended Analyses for Sea Surface Temperature. *J. Clim.* **20**, 5473–5496 (2007).

85. Johannessen, O. *et al.* Arctic climate change: observed and modelled temperature and sea-ice variability. *Tellus A Dyn. Meteorol. Oceanogr.* **56**, 328–341 (2004).

86. Hijmans, R. J. *et al.* raster: Geographic data analysis and modelling. (2020).

87. Roger, A., Stuetz, R., Ove, K., Giraudoux, P. & Santilli, S. rgeos: Interface to geometry engine - open. (2020).

88. Detrich, H. W., Parker, S. K., Williams, J., Nogales, E. & Downing, K. H. Cold adaptation of microtubule assembly and dynamics. Structural interpretation of primary sequence changes present in the α- and β-tubulins of antarctic fishes. *J. Biol. Chem.* **275**, 37038–37047 (2000).

89. Cheng, C. H. C. & Detrich, H. W. Molecular ecophysiology of Antarctic notothenioid fishes. *Philos. Trans. R. Soc. B Biol. Sci.* **362**, 2215–2232 (2007).

90. Shin, S. C. hu. *et al.* The genome sequence of the Antarctic bullhead notothen reveals evolutionary adaptations to a cold environment. *Genome Biol.* **15**, 468 (2014).

91. Environmental Systems Research Institute. ArcGIS Desktop: Release 10.8. (2017).

Acknowledgments

The authors acknowledge that the species collections took place on Huu-ay-aht and Sechelt First Nations traditional territories and are grateful for the opportunity to conduct their research in protected and sacred areas. We would like to thank the Bamfield Marine Sciences Centre for the resources required to conduct this research, Sam Owens for the photo in Figure 1a, Peter Peller for creating Figure 1b, as well as Daniel Wuitchik, Sam Yeaman, Jennifer Sunday, and Patrick Nosil for feedback on the manuscript.

558 **Author Contributions**

559 This study was designed by SJSW, RDHB, and SMR; fish husbandry and breeding by SJSW and

560 TNB; experimental data collection by SJSW; DNA sequencing and initial processing by AP;

561 bioinformatic and QTL analyses by SJSW; species distribution modelling by SJSW and SM; the

562 manuscript was written by SJSW, RDHB, and SMR, with input from authors; the study was

563 funded by HAJ, RDHB, and SMR.

564

565 Competing Interests: The authors declare no competing interests.

566

567

## Figures and Tables

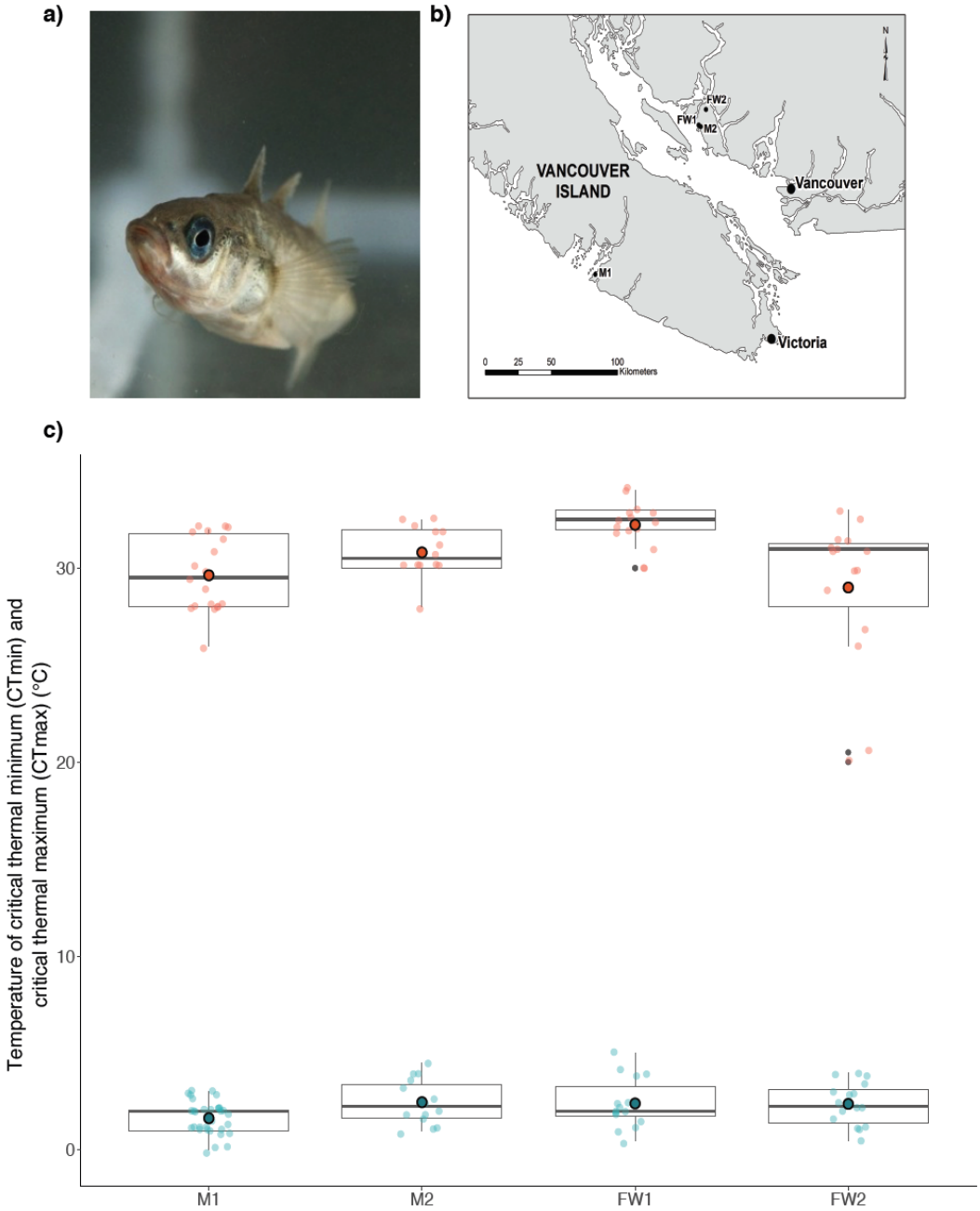


**Figure 1.** a) Adult threespine stickleback (*Gasterosteus aculeatus*) from a single genetic cluster were sampled from b) two marine and two freshwater populations in the Canadian Pacific Northwest. These populations were assayed for c) critical thermal minima and maxima. Thermal trait values for marine populations (M1 and M2) were incorporated into the species distribution models, while marine and freshwater populations (M1, FW1, and FW2) were used to generate F1 and F2 generations for linkage map construction and quantitative trait loci (QTL) analyses.

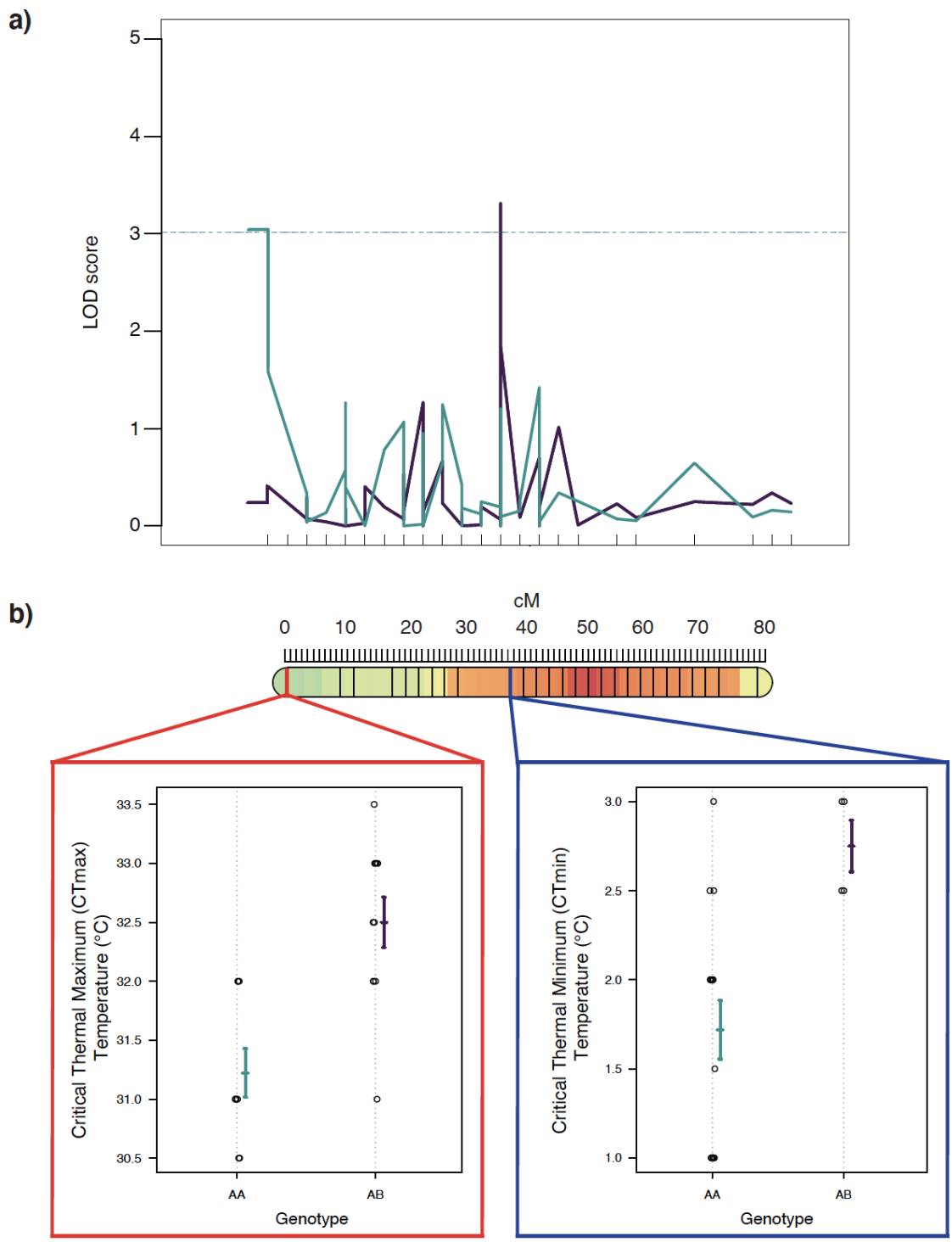


**Figure 2.** a) Quantitative trait loci (QTL) scan of linkage group 4 with trait-specific significance thresholds for LOD scores, showing a significant LOD peak for CTmin (dark purple) and CTmax (light blue) with b) an inset of linkage group 4 highlighting the position of the significant QTL for upper and lower thermal tolerances (CTmax and CTmin, respectively).

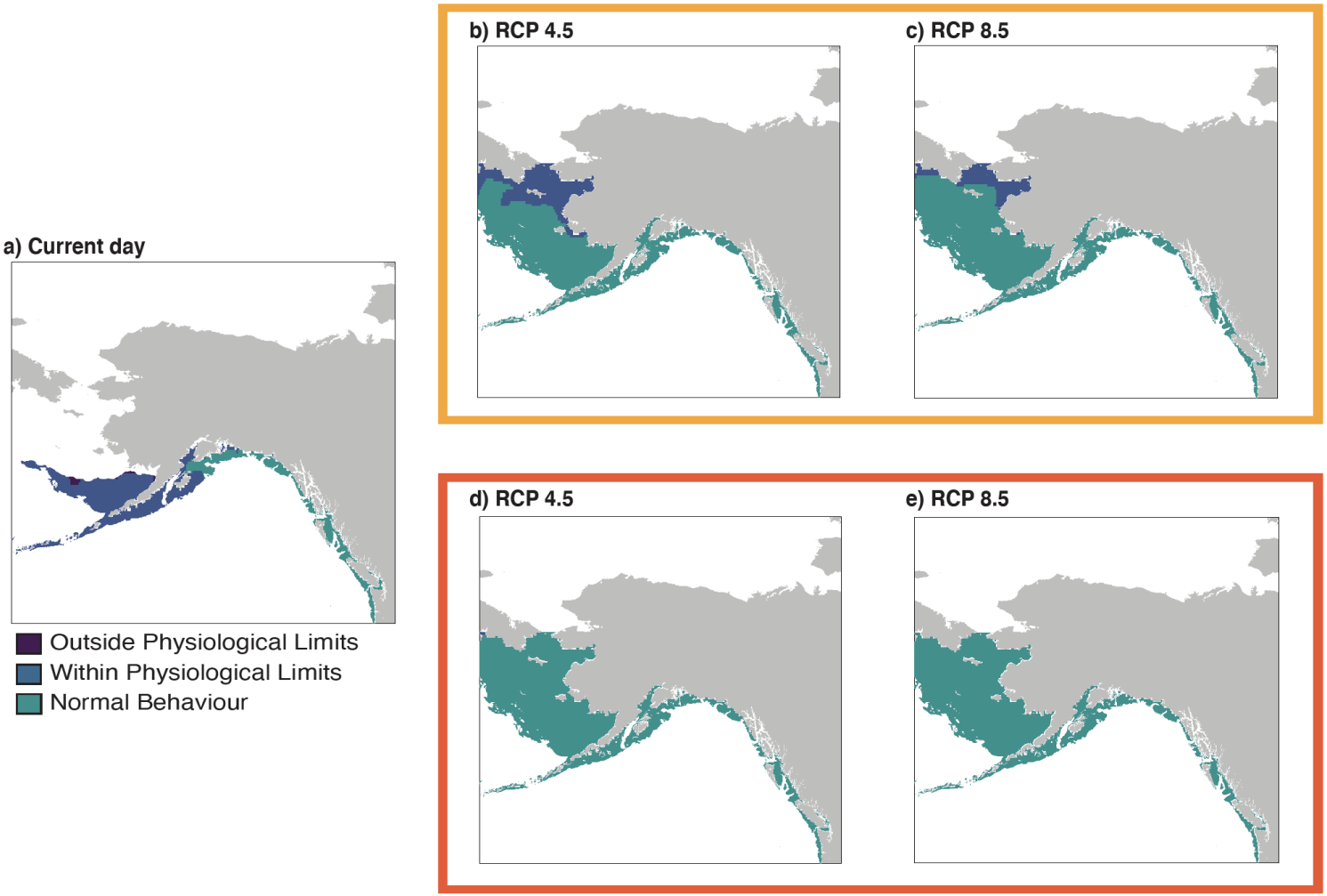


**Figure 3.** Changes in the distribution of marine threespine stickleback (*Gasterosteus aculeatus*) as a result of incorporating thermal traits in a) current day environmental conditions and under IPCC end-of-century projections RCP 4.5 and 8.5 without trait evolution ('no evolution' model, b & c, orange box) and with trait evolution ('evolution' model, d & e, red box)**.**

**Supplementary Figures and Tables**

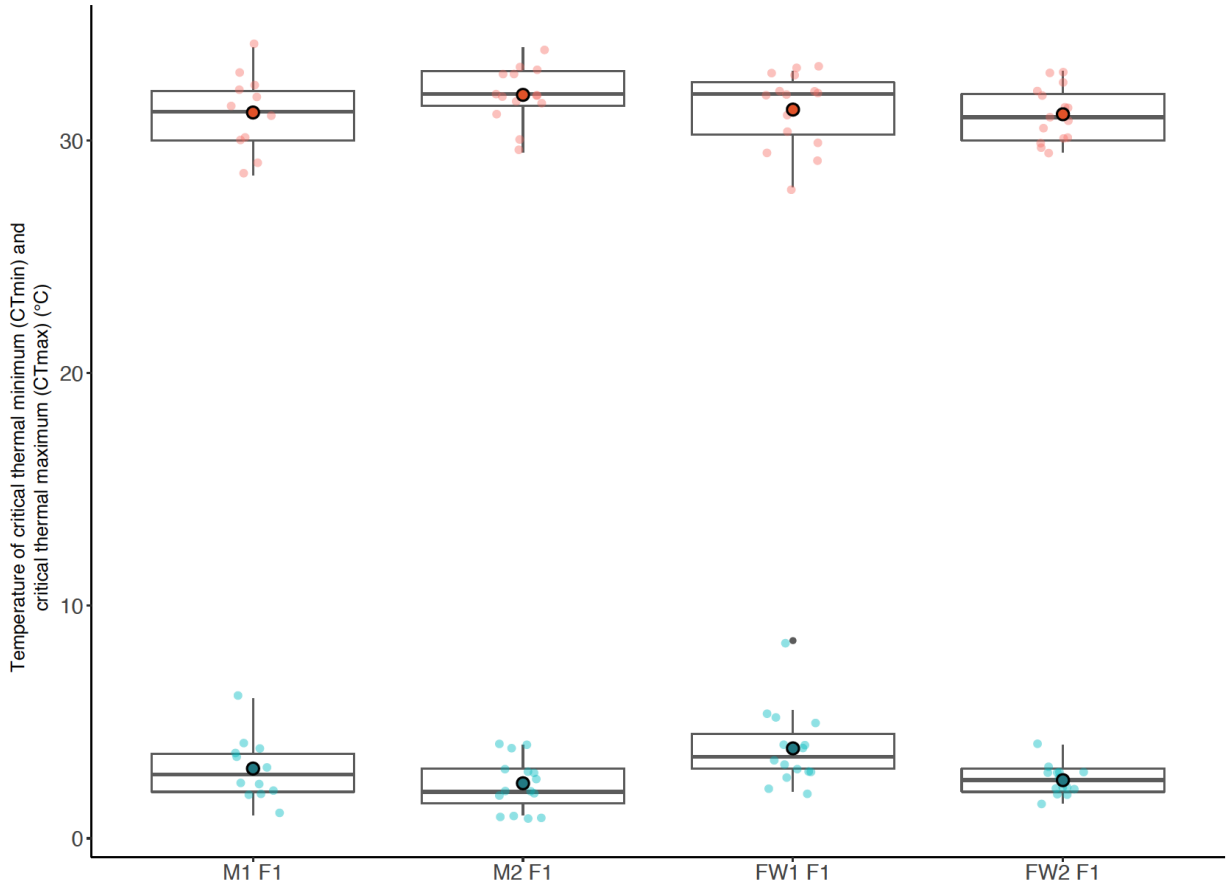


**Figure S1.** Critical thermal minimum (CTmin) and maximum (CTmax) measurements for adult threespine stickleback (*Gasterosteus aculeatus*) from pure F1 marine (M*F1) and freshwater (FW*F1) families raised in a common garden under a constant thermal environment.

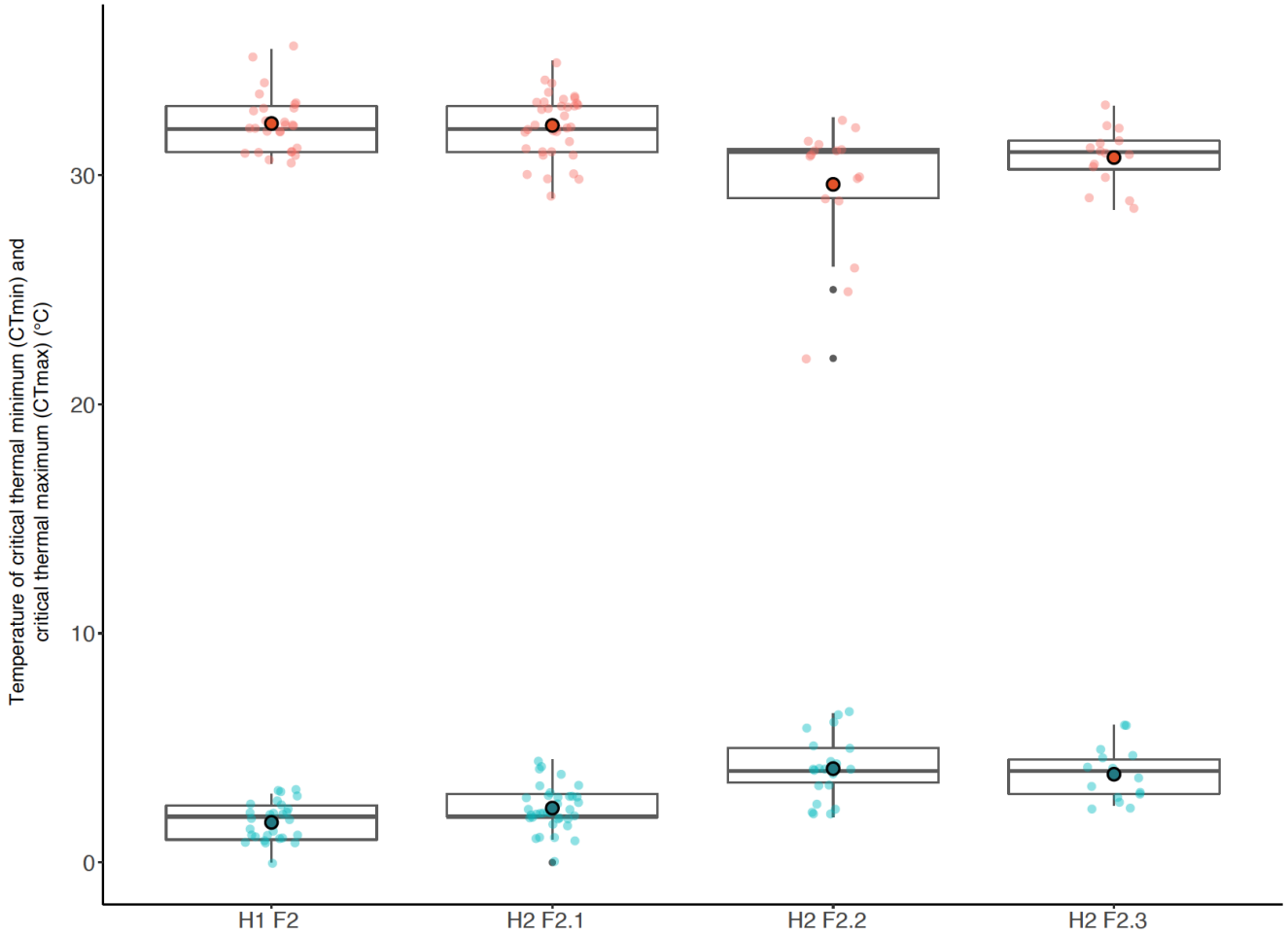


**Figure S2.** Critical thermal minimum (CTmin) and maximum (CTmax) measurements for adult threespine stickleback (*Gasterosteus aculeatus*) from hybrid marine-freshwater F2 families raised in a common garden under a constant thermal environment.

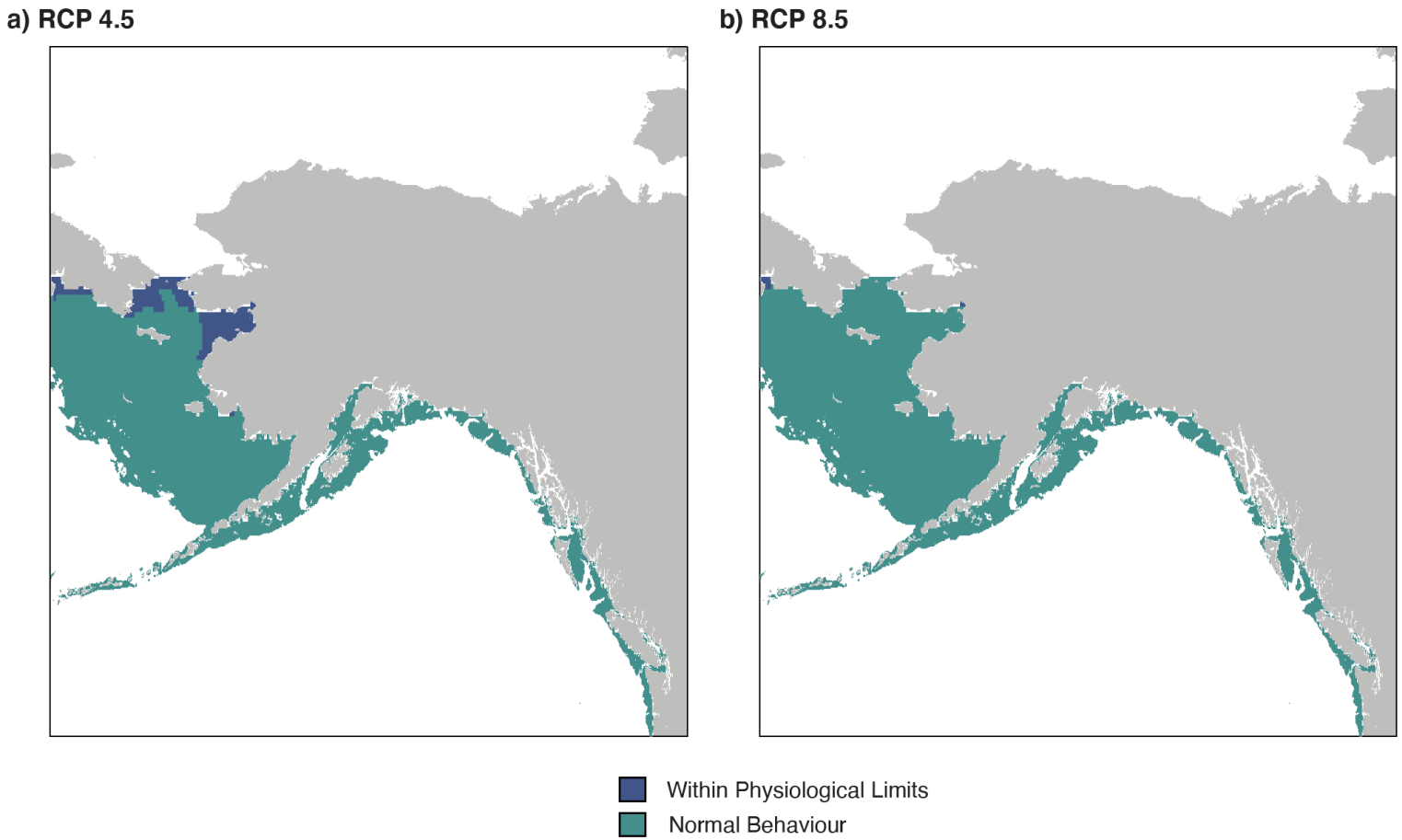


**Figure S3.** Changes in the distribution of marine threespine stickleback (*Gasterosteus aculeatus*) as a result of incorporating thermal traits under IPCC end-of-century projections RCP 4.5 and 8.5 with trait evolution constrained by the underlying genetic architecture of critical thermal minimum (CTmin) as determined from hybrid F2 mapping families.

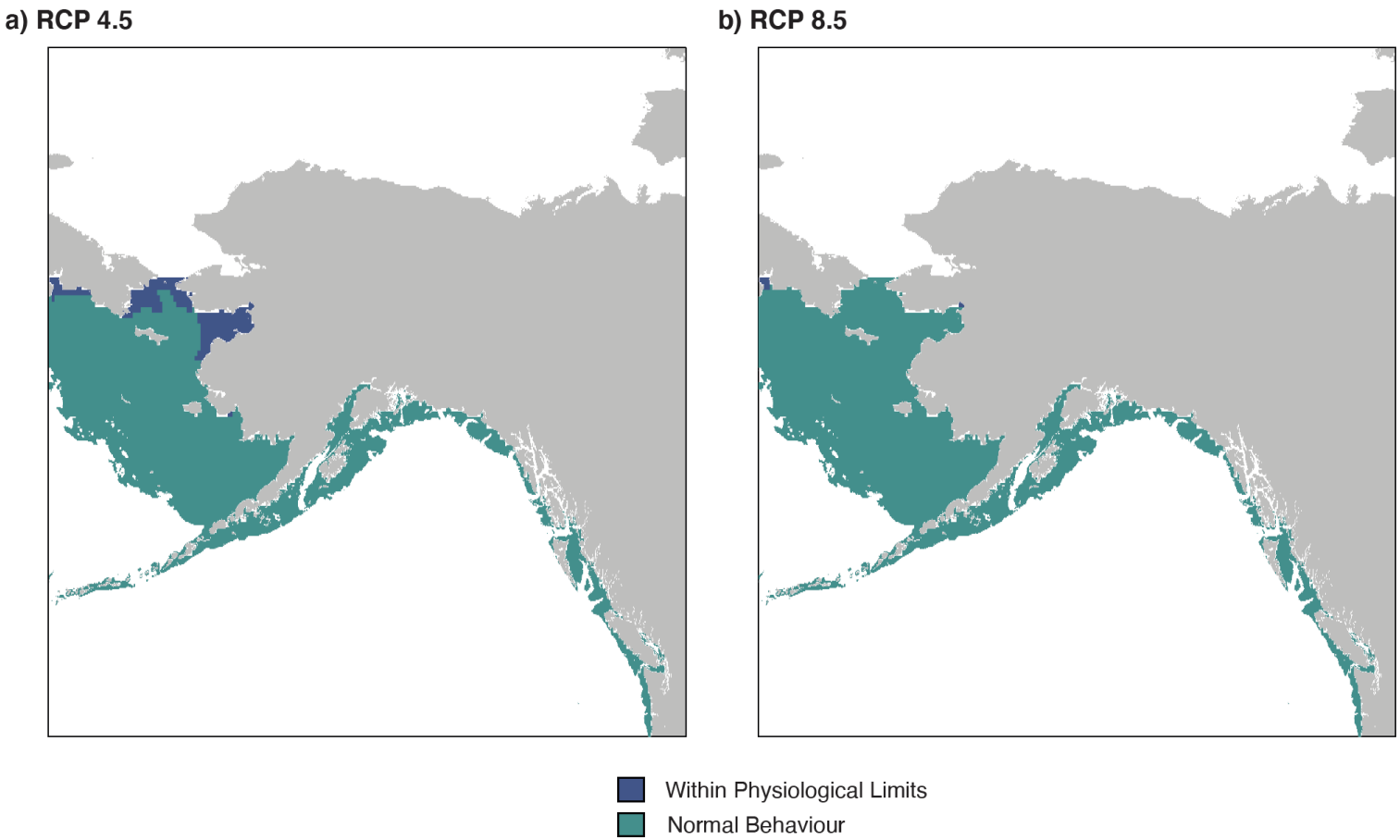


**Figure S4.** Changes in the distribution of marine threespine stickleback (*Gasterosteus aculeatus*) as a result of incorporating thermal traits under IPCC end-of-century projections RCP 4.5 and 8.5 with trait evolution constrained by the underlying genetic architecture of critical thermal minimum (CTmin) and critical thermal maximum (CTmax) as determined from hybrid F2 mapping families.

**Table S1.** Summaries of family-specific linkage maps constructed for quantitative trait loci (QTL) analyses.

| **Map** | $n_{markers}$ | **Length (cM)** | **Avg. Max. Spacing** |
|---|---|---|---|
| KL1 | 2139 | 1370.4 | 7.6 |
| KL2 | 1558 | 1311 | 8.5 |
| KL3 | 1964 | 1359.5 | 7.9 |
| HL | 5247 | 1621.1 | 11.8 |

**Table S2.** Thermal trait data from *Gasterosteus aculeatus* used to inform the species distribution envelopes (rows) in the varied evolutionary scenarios (columns) projected for end-of-century conditions.

| | Current day | No evolution | Adjusted PVE | Evolution |
|---|---|---|---|---|
| Normal Behaviour | (5 - 25) | (5 - 25) | (3.6 - 25) | (2.5 - 25) |
| Within Physiological Limits | (0.9 - 31.9) | (0.9 - 31.9) | (0 - 31.9) | (0 - 31.9) |
| Outside Physiological Limits | $31.9 > x < 0.9$ | $31.9 > x < 0.9$ | $31.9 > x < 0$ | $31.9 > x < 0$ |